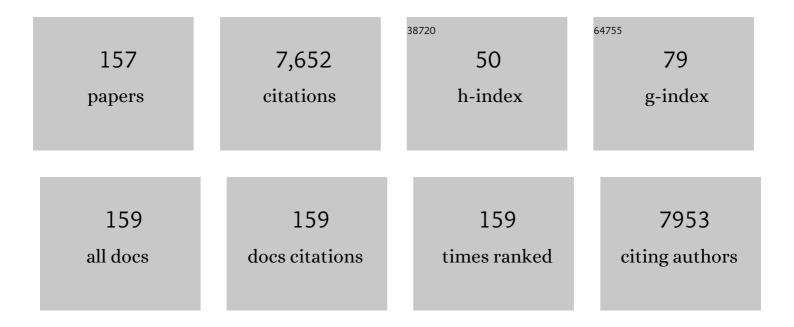
Kyriaki Polychronopoulou

List of Publications by Year in descending order

Source: https://exaly.com/author-pdf/2741494/publications.pdf Version: 2024-02-01



#	Article	IF	CITATIONS
1	Carbon Aerogel from Winter Melon for Highly Efficient and Recyclable Oils and Organic Solvents Absorption. ACS Sustainable Chemistry and Engineering, 2014, 2, 1492-1497.	3.2	296
2	Thermal and chemical stability of hexagonal boron nitride (h-BN) nanoplatelets. Vacuum, 2015, 112, 42-45.	1.6	236
3	From biomass to high performance solar–thermal and electric–thermal energy conversion and storage materials. Journal of Materials Chemistry A, 2014, 2, 7759-7765.	5.2	213
4	Chalcogenide Aerogels as Sorbents for Radioactive Iodine. Chemistry of Materials, 2015, 27, 2619-2626.	3.2	186
5	Adaptive VN/Ag nanocomposite coatings with lubricious behavior from 25 to 1000°C. Acta Materialia, 2010, 58, 5326-5331.	3.8	177
6	An in depth investigation of deactivation through carbon formation during the biogas dry reforming reaction for Ni supported on modified with CeO2 and La2O3 zirconia catalysts. International Journal of Hydrogen Energy, 2018, 43, 18955-18976.	3.8	165
7	Porous cationic polymers: the impact of counteranions and charges on CO ₂ capture and conversion. Chemical Communications, 2016, 52, 934-937.	2.2	162
8	Chalcogen-Based Aerogels As Sorbents for Radionuclide Remediation. Environmental Science & Technology, 2013, 47, 7540-7547.	4.6	161
9	Lightweight and Highly Conductive Aerogel-like Carbon from Sugarcane with Superior Mechanical and EMI Shielding Properties. ACS Sustainable Chemistry and Engineering, 2015, 3, 1419-1427.	3.2	160
10	Highly selective and stable nickel catalysts supported on ceria promoted with Sm2O3, Pr2O3 and MgO for the CO2 methanation reaction. Applied Catalysis B: Environmental, 2021, 282, 119562.	10.8	149
11	Nano-zerovalent manganese/biochar composite for the adsorptive and oxidative removal of Congo-red dye from aqueous solutions. Journal of Hazardous Materials, 2021, 403, 123854.	6.5	144
12	High entropy oxides-exploring a paradigm of promising catalysts: A review. Materials and Design, 2021, 202, 109534.	3.3	140
13	Ni supported on CaO-MgO-Al2O3 as a highly selective and stable catalyst for H2 production via the glycerol steam reforming reaction. International Journal of Hydrogen Energy, 2019, 44, 256-273.	3.8	138
14	The phenol steam reforming reaction over MgO-based supported Rh catalysts. Journal of Catalysis, 2004, 228, 417-432.	3.1	136
15	Absorption-enhanced reforming of phenol by steam over supported Fe catalysts. Journal of Catalysis, 2006, 241, 132-148.	3.1	129
16	Investigating the correlation between deactivation and the carbon deposited on the surface of Ni/Al2O3 and Ni/La2O3-Al2O3 catalysts during the biogas reforming reaction. Applied Surface Science, 2019, 474, 42-56.	3.1	128
17	An Investigation of the NO/H2/O2 (Lean De-NOx) Reaction on a Highly Active and Selective Pt/La0.7Sr0.2Ce0.1FeO3 Catalyst at Low Temperatures. Journal of Catalysis, 2002, 209, 456-471.	3.1	123
18	Highly Hydrophobic ZIFâ€8/Carbon Nitride Foam with Hierarchical Porosity for Oil Capture and Chemical Fixation of CO ₂ . Advanced Functional Materials, 2017, 27, 1700706.	7.8	119

#	Article	IF	CITATIONS
19	Nanoporous Polymers Incorporating Sterically Confined <i>N</i> -Heterocyclic Carbenes for Simultaneous CO ₂ Capture and Conversion at Ambient Pressure. Chemistry of Materials, 2015, 27, 6818-6826.	3.2	116
20	Multifunctional redox-tuned viologen-based covalent organic polymers. Journal of Materials Chemistry A, 2016, 4, 15361-15369.	5.2	114
21	Synergistic effects of activated carbon and nano-zerovalent copper on the performance of hydroxyapatite-alginate beads for the removal of As3+ from aqueous solution. Journal of Cleaner Production, 2019, 235, 875-886.	4.6	108
22	Nanoporous activated carbon cloth as a versatile material for hydrogen adsorption, selective gas separation and electrochemical energy storage. Nano Energy, 2017, 40, 49-64.	8.2	101
23	Hydrogen production via the glycerol steam reforming reaction over nickel supported on alumina and lanthana-alumina catalysts. International Journal of Hydrogen Energy, 2017, 42, 13039-13060.	3.8	100
24	The steam reforming of phenol reaction over supported-Rh catalysts. Applied Catalysis A: General, 2004, 272, 37-52.	2.2	93
25	Novel Zn–Ti-based mixed metal oxides for low-temperature adsorption of H2S from industrial gas streams. Applied Catalysis B: Environmental, 2005, 57, 125-137.	10.8	92
26	Chemical Blowing Approach for Ultramicroporous Carbon Nitride Frameworks and Their Applications in Gas and Energy Storage. Advanced Functional Materials, 2017, 27, 1604658.	7.8	92
27	Ni/Y2O3–ZrO2 catalyst for hydrogen production through the glycerol steam reforming reaction. International Journal of Hydrogen Energy, 2020, 45, 10442-10460.	3.8	85
28	Glycerol Steam Reforming for Hydrogen Production over Nickel Supported on Alumina, Zirconia and Silica Catalysts. Topics in Catalysis, 2017, 60, 1226-1250.	1.3	79
29	Highly selective and stable Ni/La-M (M=Sm, Pr, and Mg)-CeO2 catalysts for CO2 methanation. Journal of CO2 Utilization, 2021, 51, 101618.	3.3	78
30	Synthesis of hierarchical porous Zeolite-Y for enhanced CO2 capture. Microporous and Mesoporous Materials, 2020, 303, 110261.	2.2	73
31	The Relationship between Reaction Temperature and Carbon Deposition on Nickel Catalysts Based on Al2O3, ZrO2 or SiO2 Supports during the Biogas Dry Reforming Reaction. Catalysts, 2019, 9, 676.	1.6	72
32	Novel Fe–Mn–Zn–Ti–O mixed-metal oxides for the low-temperature removal of H2S from gas streams in the presence of H2, CO2, and H2O. Journal of Catalysis, 2005, 236, 205-220.	3.1	71
33	The potential of glycerol and phenol towards H2 production using steam reforming reaction: A review. Surface and Coatings Technology, 2018, 352, 92-111.	2.2	71
34	Design Aspects of Doped CeO ₂ for Low-Temperature Catalytic CO Oxidation: Transient Kinetics and DFT Approach. ACS Applied Materials & Interfaces, 2021, 13, 22391-22415.	4.0	70
35	Synthesis and performance evaluation of hydrocracking catalysts: A review. Journal of Industrial and Engineering Chemistry, 2020, 89, 83-103.	2.9	68
36	The influence of SiO2 doping on the Ni/ZrO2 supported catalyst for hydrogen production through the glycerol steam reforming reaction. Catalysis Today, 2019, 319, 206-219.	2.2	67

#	Article	IF	CITATIONS
37	Deep eutectic solvent-mediated synthesis of ceria nanoparticles with the enhanced yield for photocatalytic degradation of flumequine under UV-C. Journal of Water Process Engineering, 2020, 33, 101012.	2.6	67
38	Electrodeposited Nanostructured CoFe2O4 for Overall Water Splitting and Supercapacitor Applications. Catalysts, 2019, 9, 176.	1.6	65
39	Effect of operating parameters on the selective catalytic deoxygenation of palm oil to produce renewable diesel over Ni supported on Al2O3, ZrO2 and SiO2 catalysts. Fuel Processing Technology, 2020, 209, 106547.	3.7	65
40	Synthesis of nitrogen-doped Ceria nanoparticles in deep eutectic solvent for the degradation of sulfamethaxazole under solar irradiation and additional antibacterial activities. Chemical Engineering Journal, 2020, 394, 124869.	6.6	65
41	Selective Surfaces: Quaternary Co(Ni)MoS-Based Chalcogels with Divalent (Pb ²⁺ ,) Tj ETQq1 1 0.784 Separation. Chemistry of Materials, 2012, 24, 3380-3392.	1314 rgBT 3.2	/Overlock 10 63
42	Rapid microwave assisted sol-gel synthesis of CeO2 and CexSm1-xO2 nanoparticle catalysts for CO oxidation. Molecular Catalysis, 2017, 428, 41-55.	1.0	62
43	Nano zerovalent zinc catalyzed peroxymonosulfate based advanced oxidation technologies for treatment of chlorpyrifos in aqueous solution: A semi-pilot scale study. Journal of Cleaner Production, 2020, 246, 119032.	4.6	62
44	Solar light responsive bismuth doped titania with Ti3+ for efficient photocatalytic degradation of flumequine: Synergistic role of peroxymonosulfate. Chemical Engineering Journal, 2020, 384, 123255.	6.6	62
45	Nanostructure, mechanical and tribological properties of reactive magnetron sputtered TiCx coatings. Diamond and Related Materials, 2008, 17, 2054-2061.	1.8	61
46	Reduced Graphene Oxide: Effect of Reduction on Electrical Conductivity. Journal of Composites Science, 2018, 2, 25.	1.4	61
47	Cu, Sm co-doping effect on the CO oxidation activity of CeO2. A combined experimental and density functional study. Applied Surface Science, 2020, 521, 146305.	3.1	61
48	The role of oxygen and hydroxyl support species on the mechanism of H2 production in the steam reforming of phenol over metal oxide-supported-Rh and -Fe catalysts. Catalysis Today, 2006, 112, 89-93.	2.2	60
49	Morphology-dependent electrochemical performance of MnO2 nanostructures on graphene towards efficient capacitive deionization. Electrochimica Acta, 2020, 330, 135202.	2.6	55
50	Tailoring MgO-based supported Rh catalysts for purification of gas streams from phenol. Applied Catalysis B: Environmental, 2012, 111-112, 360-375.	10.8	52
51	Spillover of labile OH, H, and O species in the H2 production by steam reforming of phenol over supported-Rh catalysts. Catalysis Today, 2006, 116, 341-347.	2.2	50
52	A DFT study of the adsorption energy and electronic interactions of the SO ₂ molecule on a CoP hydrotreating catalyst. RSC Advances, 2021, 11, 2947-2957.	1.7	49
53	Water–Gas Shift Reaction on Pt/Ce _{1–<i>x</i>} Ti _{<i>x</i>} O _{2â^î^} : The Effect of Ce/Ti Ratio. Journal of Physical Chemistry C, 2013, 117, 25467-25477.	1.5	48
54	Nano-zerovalent copper as a Fenton-like catalyst for the degradation of ciprofloxacin in aqueous solution. Journal of Water Process Engineering, 2020, 37, 101325.	2.6	48

#	Article	IF	CITATIONS
55	Promoting effect of CaO-MgO mixed oxide on Ni/γ-Al2O3 catalyst for selective catalytic deoxygenation of palm oil. Renewable Energy, 2020, 162, 1793-1810.	4.3	47
56	Synthesis of Highly Porous Coordination Polymers with Open Metal Sites for Enhanced Gas Uptake and Separation. ACS Applied Materials & Interfaces, 2016, 8, 26860-26867.	4.0	46
57	Highly Electrically Conductive Nanocomposites Based on PolymerInfused Graphene Sponges. Scientific Reports, 2014, 4, 4652.	1.6	45
58	Room temperature synthesis and high temperature frictional study of silver vanadate nanorods. Nanotechnology, 2010, 21, 325601.	1.3	40
59	The significance of tribochemistry on the performance of PTFE-based coatings in CO2 refrigerant environment. Surface and Coatings Technology, 2009, 204, 319-329.	2.2	39
60	Calix[4]arene-Based Porous Organic Nanosheets. ACS Applied Materials & Interfaces, 2018, 10, 17359-17365.	4.0	39
61	Nickel Supported on AlCeO3 as a Highly Selective and Stable Catalyst for Hydrogen Production via the Glycerol Steam Reforming Reaction. Catalysts, 2019, 9, 411.	1.6	39
62	Cu-Ce-La-Ox as efficient CO oxidation catalysts: Effect of Cu content. Applied Surface Science, 2020, 505, 144474.	3.1	39
63	Recent Advances in Metal-Catalyzed Alkyl–Boron (C(sp3)–C(sp2)) Suzuki-Miyaura Cross-Couplings. Catalysts, 2020, 10, 296.	1.6	39
64	Microporous Elastomer Filter Coated with Metal Organic Frameworks for Improved Selectivity and Stability of Metal Oxide Gas Sensors. ACS Applied Materials & Interfaces, 2020, 12, 13338-13347.	4.0	39
65	Three-body abrasive wear by (silica) sand of advanced polymeric coatings for tilting pad bearings. Wear, 2017, 382-383, 40-50.	1.5	38
66	Hierarchical AlPO4-5 and SAPO-5 microporous molecular sieves with mesoporous connectivity for water sorption applications. Surface and Coatings Technology, 2018, 353, 378-386.	2.2	37
67	Development of novel surfactant functionalized porous graphitic carbon as an efficient adsorbent for the removal of methylene blue dye from aqueous solutions. Journal of Water Process Engineering, 2019, 28, 69-81.	2.6	37
68	Optimizing the oxide support composition in Pr-doped CeO2 towards highly active and selective Ni-based CO2 methanation catalysts. Journal of Energy Chemistry, 2022, 71, 547-561.	7.1	36
69	Effects of Solâ^'Gel Synthesis on 5Feâ^'15Mnâ^'40Znâ^'40Tiâ^'O Mixed Oxide Structure and its H ₂ S Removal Efficiency from Industrial Gas Streams. Environmental Science & Technology, 2009, 43, 4367-4372.	4.6	34
70	Ce–Sm– <i>x</i> Cu cost-efficient catalysts for H ₂ production through the glycerol steam reforming reaction. Sustainable Energy and Fuels, 2019, 3, 673-691.	2.5	34
71	The nanostructure, wear and corrosion performance of arc-evaporated CrBxNy nanocomposite coatings. Surface and Coatings Technology, 2009, 204, 246-255.	2.2	33
72	Tribological study of high bearing blended polymer-based coatings for air-conditioning and refrigeration compressors. Surface and Coatings Technology, 2011, 205, 2994-3005.	2.2	33

#	Article	IF	CITATIONS
73	Ultrasmall Metal-Doped CeO ₂ Nanoparticles for Low-Temperature CO Oxidation. ACS Applied Nano Materials, 2020, 3, 10805-10813.	2.4	33
74	Insights into the thermal stability and conversion of carbon-based materials by using ReaxFF reactive force field: Recent advances and future directions. Carbon, 2022, 196, 840-866.	5.4	32
75	Textured VN coatings with Ag3VO4 solid lubricant reservoirs. Surface and Coatings Technology, 2011, 206, 1932-1935.	2.2	31
76	Cu-Ce-O catalyst revisited for exceptional activity at low temperature CO oxidation reaction. Surface and Coatings Technology, 2018, 354, 313-323.	2.2	31
77	Synthesis of nanoporous graphene oxide adsorbents by freeze-drying or microwave radiation: Characterization and hydrogen storage properties. International Journal of Hydrogen Energy, 2015, 40, 6844-6852.	3.8	30
78	Activated Carbon Derived from <i>Phoenix dactylifera</i> (Palm Tree) and Decorated with MnO ₂ Nanoparticles for Enhanced Hybrid Capacitive Deionization Electrodes. ChemistrySelect, 2020, 5, 3248-3256.	0.7	29
79	Adsorption of Hydrogen Sulfide at Low Temperatures Using an Industrial Molecular Sieve: An Experimental and Theoretical Study. ACS Omega, 2021, 6, 14774-14787.	1.6	29
80	Catalytic fast pyrolysis of agricultural residues and dedicated energy crops for the production of high energy density transportation biofuels. Part I: Chemical pathways and bio-oil upgrading. Renewable Energy, 2022, 185, 483-505.	4.3	29
81	Tribological performance comparing different refrigerant–lubricant systems: The case of environmentally friendly HFO-1234yf refrigerant. Tribology International, 2014, 78, 176-186.	3.0	28
82	Solvothermal synthesis, nanostructural characterization and gas cryo-adsorption studies in a metal–organic framework (IRMOF-1) material. International Journal of Hydrogen Energy, 2017, 42, 23899-23907.	3.8	28
83	Tailoring the efficiency of an active catalyst for CO abatement through oxidation reaction: The case study of samarium-doped ceria. Journal of Environmental Chemical Engineering, 2018, 6, 266-280.	3.3	28
84	Lubricity of environmentally friendly HFO-1234yf refrigerant. Tribology International, 2013, 57, 92-100.	3.0	27
85	High temperature nanotribology of ultra-thin hydrogenated amorphous carbon coatings. Carbon, 2017, 123, 112-121.	5.4	27
86	The Effect of WO3 Modification of ZrO2 Support on the Ni-Catalyzed Dry Reforming of Biogas Reaction for Syngas Production. Frontiers in Environmental Science, 2017, 5, .	1.5	26
87	A comparative study of Ni catalysts supported on Al2O3, MgO–CaO–Al2O3 and La2O3–Al2O3 for the dry reforming of ethane. International Journal of Hydrogen Energy, 2022, 47, 5337-5353.	3.8	26
88	Tuning the activity of Cu-containing rare earth oxide catalysts for CO oxidation reaction: Cooling while heating paradigm in microwave-assisted synthesis. Materials Research Bulletin, 2018, 108, 142-150.	2.7	25
89	Ceria-Based Materials for Hydrogen Production Via Hydrocarbon Steam Reforming and Water-Gas Shift Reactions. Recent Patents on Materials Science, 2011, 4, 122-145.	0.5	25
90	Novel CeO2-based screen-printed potentiometric electrodes for pH monitoring. Talanta, 2011, 87, 126-135.	2.9	24

#	Article	IF	CITATIONS
91	The Effect of Ni Addition onto a Cu-Based Ternary Support on the H2 Production over Glycerol Steam Reforming Reaction. Nanomaterials, 2018, 8, 931.	1.9	24
92	Solventâ€Influenced Fragmentations in Freeâ€Standing Threeâ€Dimensional Covalent Organic Framework Membranes for Hydrophobicity Switching. Angewandte Chemie - International Edition, 2022, 61, .	7.2	24
93	Low-temperature catalytic decomposition of ethylene into H2 and secondary carbon nanotubes over Ni/CNTs. Applied Catalysis B: Environmental, 2010, 93, 314-324.	10.8	23
94	Nanoporous spongy graphene: Potential applications for hydrogen adsorption and selective gas separation. Thin Solid Films, 2015, 596, 242-249.	0.8	23
95	Few-step synthesis, thermal purification and structural characterization of porous boron nitride nanoplatelets. Materials and Design, 2016, 110, 540-548.	3.3	23
96	Ni Catalysts Based on Attapulgite for Hydrogen Production through the Glycerol Steam Reforming Reaction. Catalysts, 2019, 9, 650.	1.6	23
97	NOx Control via H2-Selective Catalytic Reduction (H2-SCR) Technology for Stationary and Mobile Applications. Recent Patents on Materials Science, 2012, 5, 87-104.	0.5	23
98	Elucidating the role of La3+/Sm3+ in the carbon paths of dry reforming of methane over Ni/Ce-La(Sm)-Cu-O using transient kinetics and isotopic techniques. Applied Catalysis B: Environmental, 2022, 304, 121015.	10.8	23
99	Synthesis of nanoporous zeolite-Y and zeolite-Y/GO nanocomposite using polyelectrolyte functionalized graphene oxide. Surface and Coatings Technology, 2018, 350, 369-375.	2.2	22
100	A Review on New 3-D Printed Materials' Geometries for Catalysis and Adsorption: Paradigms from Reforming Reactions and CO2 Capture. Nanomaterials, 2020, 10, 2198.	1.9	22
101	Nanostructured Fe-Ni Sulfide: A Multifunctional Material for Energy Generation and Storage. Catalysts, 2019, 9, 597.	1.6	21
102	Continuous selective deoxygenation of palm oil for renewable diesel production over Ni catalysts supported on Al ₂ O ₃ and La ₂ O ₃ –Al ₂ O ₃ . RSC Advances, 2021, 11, 8569-8584.	1.7	21
103	Oxy-chlorination as an effective treatment of aged Pd/CeO2-Al2O3 catalysts for Pd redispersion. Applied Catalysis B: Environmental, 2012, 111-112, 349-359.	10.8	20
104	Synthesis and properties of 1D Sm-doped CeO2 composite nanofibers fabricated using a coupled electrospinning and sol–gel methodology. Ceramics International, 2016, 42, 10734-10744.	2.3	20
105	Mesoporous silica "plated―copper hydroxides/oxides heterostructures as superior regenerable sorbents for low temperature H2S removal. Chemical Engineering Journal, 2020, 398, 125585.	6.6	20
106	Influence of Graphene Reduction and Polymer Cross-Linking on Improving the Interfacial Properties of Multilayer Thin Films. ACS Applied Materials & Interfaces, 2017, 9, 1107-1118.	4.0	19
107	Influence of salt on nanozeolite-Y particles size synthesized under organic template-free condition. Microporous and Mesoporous Materials, 2019, 282, 73-81.	2.2	19
108	The Effect of Noble Metal (M: Ir, Pt, Pd) on M/Ce2O3-γ-Al2O3 Catalysts for Hydrogen Production via the Steam Reforming of Glycerol. Catalysts, 2020, 10, 790.	1.6	18

#	Article	IF	CITATIONS
109	Cerium oxide catalysts for oxidative coupling of methane reaction: Effect of lithium, samarium and lanthanum dopants. Journal of Environmental Chemical Engineering, 2022, 10, 107259.	3.3	18
110	Catalytic fast pyrolysis of agricultural residues and dedicated energy crops for the production of high energy density transportation biofuels. Part II: Catalytic research. Renewable Energy, 2022, 189, 315-338.	4.3	18
111	Transition Metal Phosphides (TMP) as a Versatile Class of Catalysts for the Hydrodeoxygenation Reaction (HDO) of Oil-Derived Compounds. Nanomaterials, 2022, 12, 1435.	1.9	18
112	Synthesis and characterization of Cr–B–N coatings deposited by reactive arc evaporation. Journal of Materials Research, 2008, 23, 3048-3055.	1.2	17
113	Lubricity effect of carbon dioxide used as an environmentally friendly refrigerant in air-conditioning and refrigeration compressors. Wear, 2010, 270, 46-56.	1.5	17
114	Studying the stability of Ni supported on modified with CeO2 alumina catalysts for the biogas dry reforming reaction. Materials Today: Proceedings, 2018, 5, 27607-27616.	0.9	17
115	Decoupling the Chemical and Mechanical Strain Effect on Steering the CO ₂ Activation over CeO ₂ -Based Oxides: An Experimental and DFT Approach. ACS Applied Materials & Interfaces, 2022, 14, 33094-33119.	4.0	17
116	Growth and characterization of ceria thin films and Ce-doped γ <i>-</i> Al ₂ O ₃ nanowires using sol–gel techniques. Nanotechnology, 2010, 21, 465606.	1.3	16
117	Tribological performance of environmentally friendly refrigerant HFO-1234 yf under starved lubricated conditions. Wear, 2013, 304, 191-201.	1.5	16
118	An Efficient Method to Predict Compressibility Factor of Natural Gas Streams. Energies, 2019, 12, 2577.	1.6	16
119	Photocatalytic Degradation of Ethiofencarb by a Visible Light-Driven SnIn4S8 Photocatalyst. Nanomaterials, 2021, 11, 1325.	1.9	16
120	Hydrogen production via steam reforming of glycerol over Ce-La-Cu-O ternary oxide catalyst: An experimental and DFT study. Applied Surface Science, 2022, 586, 152798.	3.1	16
121	Tribological Study Comparing PAG and POE Lubricants Used in Air-Conditioning Compressors under the Presence of CO ₂ . Tribology Transactions, 2008, 51, 790-797.	1.1	15
122	Comparative scuffing performance and chemical analysis of metallic surfaces for air-conditioning compressors in the presence of environmentally friendly CO2 refrigerant. Wear, 2010, 268, 668-676.	1.5	15
123	Low-temperature water-gas shift on Pt/Ce0.8La0.2O2â^î′–CNT: The effect of Ce0.8La0.2O2â^îſ/CNT ratio. Applied Catalysis A: General, 2015, 504, 585-598.	2.2	15
124	Transition metal complex directed synthesis of porous cationic polymers for efficient CO2 capture and conversion. Polymer, 2017, 126, 296-302.	1.8	15
125	Nanomechanical and nanotribological behaviors of hafnium boride thin films. Thin Solid Films, 2015, 595, 84-91.	0.8	14
126	Ni ₂ P Nanoparticles Embedded in Mesoporous SiO ₂ for Catalytic Hydrogenation of SO ₂ to Elemental S. ACS Applied Nano Materials, 2021, 4, 5665-5676.	2.4	14

#	Article	IF	CITATIONS
127	Silver Nanoparticle‣oaded Contact Lenses for Blueâ€Yellow Color Vision Deficiency. Physica Status Solidi (A) Applications and Materials Science, 2022, 219, 2100294.	0.8	14
128	Towards maximizing conversion of ethane and carbon dioxide into synthesis gas using highly stable Ni-perovskite catalysts. Journal of CO2 Utilization, 2022, 61, 102046.	3.3	14
129	Deposition and Nanotribological Characterization of Sub-100-nm Thick Protective Ti-Based Coatings for Miniature Applications. Tribology Letters, 2011, 44, 213-221.	1.2	13
130	Structure and mechanical properties of low temperature magnetron sputtered nanocrystalline (nc-)Ti(N,C)/amorphous diamond like carbon (a-C:H) coatings. Thin Solid Films, 2010, 519, 24-30.	0.8	12
131	Nano-architectural advancement of CeO2-driven catalysis via electrospinning. Surface and Coatings Technology, 2018, 350, 245-280.	2.2	12
132	Nickel Phosphide Nanoparticles for Selective Hydrogenation of SO ₂ to H ₂ S. ACS Applied Nano Materials, 2021, 4, 6568-6582.	2.4	11
133	Role of embedding choline chloride-urea deep eutectic solvent on biomass-derived porous activated carbon in its capacitive deionization performance. Desalination, 2022, 530, 115674.	4.0	11
134	Effect of Cu Content on the Structure, and Performance of Substoichiometric Cr–N Coatings. Tribology Letters, 2010, 38, 57-68.	1.2	10
135	Elevated-Temperature and -Pressure Tribology of Drilling Fluids Used in Oil and Gas Extended-Reach-Drilling Applications. SPE Journal, 2018, 23, 2339-2350.	1.7	10
136	Analytical model for geometrical characteristics control of laser sintered surfaces. International Journal of Nanomanufacturing, 2010, 6, 300.	0.3	9
137	Mechanical and high pressure tribological properties of nanocrystalline Ti(N,C) and amorphous C:H nanocomposite coatings. Diamond and Related Materials, 2010, 19, 960-963.	1.8	9
138	Oxidative coupling of methane on Li/CeO2 based catalysts: Investigation of the effect of Mg- and La-doping of the CeO2 support. Molecular Catalysis, 2022, 520, 112157.	1.0	9
139	Tribological Properties of Twin Electron-Beam Evaporated Cr–N and Al–Cr–N Coatings Under Laboratory Sliding and Drill Experiments. Tribology Letters, 2008, 32, 117-127.	1.2	8
140	Ceria-Based Materials for Hydrogen Production Via Hydrocarbon Steam Reforming and Water-Gas Shift Reactions. Recent Patents on Materials Science, 2011, 4, 122-145.	0.5	8
141	Polythiacalixarene-Embedded Gold Nanoparticles for Visible-Light-Driven Photocatalytic CO ₂ Reduction. ACS Applied Materials & Interfaces, 2022, 14, 30796-30801.	4.0	8
142	Shear strength measurements of hafnium diboride thin solid films. Wear, 2014, 318, 168-176.	1.5	7
143	Mercouri G. Kanatzidis: Excellence and Innovations in Inorganic and Solid-State Chemistry. Inorganic Chemistry, 2017, 56, 7582-7597.	1.9	7
144	Effect of humic acid on the solid phase stability of UO2CO3. Journal of Radioanalytical and Nuclear Chemistry, 2009, 279, 863-866.	0.7	6

#	Article	IF	CITATIONS
145	Ni/CNT/Zeolite-Y composite catalyst for efficient heptane hydrocracking: Steady-state and transient kinetic studies. Applied Catalysis A: General, 2022, 630, 118437.	2.2	6
146	Graphene Nanoplatelets-Based Ni-Zeolite Composite Catalysts for Heptane Hydrocracking. Journal of Carbon Research, 2020, 6, 31.	1.4	5
147	CO Oxidation at Near-Ambient Temperatures over TiO2-Supported Pd-Cu Catalysts: Promoting Effect of Pd-Cu Nanointerface and TiO2 Morphology. Nanomaterials, 2021, 11, 1675.	1.9	4
148	Underwater Robotic Welding of Lap Joints with Sandwiched Reactive Multilayers: Thermal, Mechanical and Material Analysis. MRS Advances, 2018, 3, 911-920.	0.5	3
149	Novel Catalytic Systems for Hydrogen Production via the Water-Gas Shift Reaction. Conference Papers in Energy, 2013, 2013, 1-8.	0.5	2
150	Nanoindentation and nanoscratch of sub-micron polymer nanocomposite films on compliant substrate. Thin Solid Films, 2021, 736, 138905.	0.8	2
151	Hierarchical structures produced using unbalanced magnetron sputtering for photocatalytic degradation of Rhodamine 6G dye. Journal of Nanoparticle Research, 2014, 16, 1.	0.8	1
152	Editorial—Special Issue "Catalysis for Energy Production― Catalysts, 2021, 11, 785.	1.6	1
153	Metal-Free Phosphated Mesoporous SiO2 as Catalyst for the Low-Temperature Conversion of SO2 to H2S in Hydrogen. Nanomaterials, 2021, 11, 2440.	1.9	1
154	Creep rupture in HP-Nb refractory steel tubes due to short-term overheating. European Journal of Materials, 2021, 1, 1-22.	0.8	1
155	Microstructure, Mechanical and Tribological Properties of Reactive Magnetron Sputtered Titanium Carbide Coatings. , 2007, , .		Ο
156	Solvent Influenced Fragmentations in Free‣tanding Threeâ€Dimensional Covalent Organic Framework Membranes for Hydrophobicity Switching. Angewandte Chemie, 0, , .	1.6	0
157	Titelbild: Solventâ€Influenced Fragmentations in Freeâ€Standing Threeâ€Dimensional Covalent Organic Framework Membranes for Hydrophobicity Switching (Angew. Chem. 13/2022). Angewandte Chemie, 2022. 134	1.6	0